Arch. Metall. Mater. **64** (2019), 2, 659-664

DOI: 10.24425/amm.2019.127595

J. SVIŽELOVÁ*#, M. TKADLEČKOVÁ*, K. MICHALEK*, J. WALEK*,
M. SATERNUS**, J. PIEPRZYCA**, T. MERDER**

NUMERICAL MODELLING OF METAL MELT REFINING PROCESS IN LADLE WITH ROTATING IMPELLER AND BREAKWATERS

The paper describes research and development of aluminium melt refining technology in a ladle with rotating impeller and breakwaters using numerical modelling of a finite volume/element method. The theoretical aspects of refining technology are outlined. The design of the numerical model is described and discussed. The differences between real process conditions and numerical model limitations are mentioned. Based on the hypothesis and the results of numerical modelling, the most appropriate setting of the numerical model is recommended. Also, the possibilities of monitoring of degassing are explained. The results of numerical modelling allow to improve the refining technology of metal melts and to control the final quality under different boundary conditions, such as rotating speed, shape and position of rotating impeller, breakwaters and intensity of inert gas blowing through the impeller.

Keywords: aluminium, refining, numerical modelling, rotating impeller, degassing

1. Introduction

Although considerable progress has been made in metallurgy over the last decades, much attention is still paid to optimisation of metallurgical processes. The technologies of refining liquid metals are no exception. It is often possible to achieve significant financial savings by reducing the refining time and by intensifying its progress. The presence of unwanted phases in molten metal can cause a number of changes in final castings, such as porosity, corrosion, reduction of electrical and thermal conductivity, etc. These phases are represented particularly by harmful gases (H) and non-metallic inclusions [1,2].

In practice, the frequently used technique for removing dissolved hydrogen and solid impurities from aluminium melt is blowing of inert gas. The process of aluminium refining by blowing inert gas can be performed in continuous and ladle reactors.

The submerged degassing device (see Fig. 1) is largely used for degassing of the metal melt in the ladle [3-6]. The submerged device consists of a hollow rotor by which the refining gas is blown into the melt. The free surface flowing and the size of the melt-atmosphere interfacial boundary can be influenced by the location of one or two breakwaters. The purpose of breakwaters is to minimise the formation of a whirl on the free surface of flowing melt during rotation of the rotor and thus to reduce the risk of further absorption of hydrogen from the surrounding atmosphere by minimising the increase of the free surface area. Due to the rotor movement, in melt volume the inert gas is dispersed into small bubbles (approx. 5 mm according to the literature [7,8]). The smaller the size of the bubble is achieved, the larger is the specific surface area of the bubbles and the degassing is more intensive. Smaller bubbles also have a longer residence time in the melt to give hydrogen more time to diffuse into the bubble [9,10].

The degassing technology using refining gas (inert or reaction gas) is based on the Sieverts Law [11]. According to the Sieverts Law, it is possible to reduce the gas content in the melt by reducing its partial pressure above the melt, as suggested by the Eq. (1). According to the literature [7], this degassing technique reduces hydrogen contents lower than 0.12 wt. % H.

$$|\%H| = \frac{K_H}{f_H}\left(p_{H_2}\right)_r \tag{1}$$

The aim of exploring this technology using numerical modelling was to deepen knowledge of the degassing process by distribution and melt flow characteristics, the behaviour of the free surface, and the determination of the velocity field. The attention will also be focused particularly on the determination of the residence times of the refining medium in the melt or verification of the character of the formed and subsequently discharged bubbles.

* VŠB-TECHNICAL UNIVERSITY OF OSTRAVA, FACULTY OF MATERIALS TECHNOLOGY, DEPARTMENT OF METALLURGY AND FOUNDRY, CZECH REPUBLIC
** SILESIAN UNIVERSITY OF TECHNOLOGY, DEPARTMENT OF EXTRACTIVE METALLURGY AND ENVIRONMENTAL PRTOTECTION, 8 KRASIŃSKIEGO STR., 40-019 KATOWICE, POLAND
# Corresponding author: jana.svizelova@vsb.cz

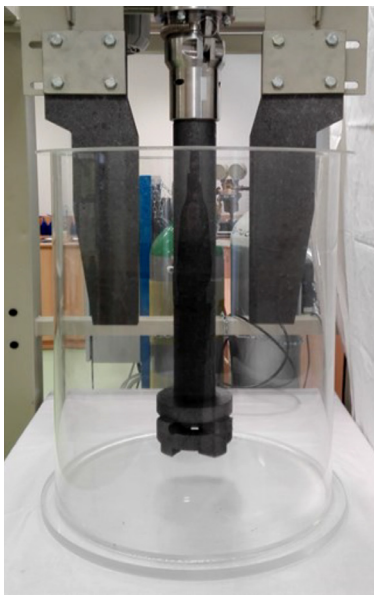

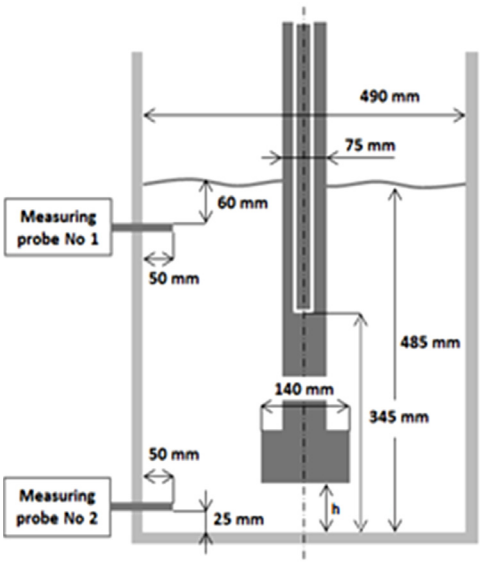

Fig. 1. Physical model of the refining ladle and its dimensions [12]

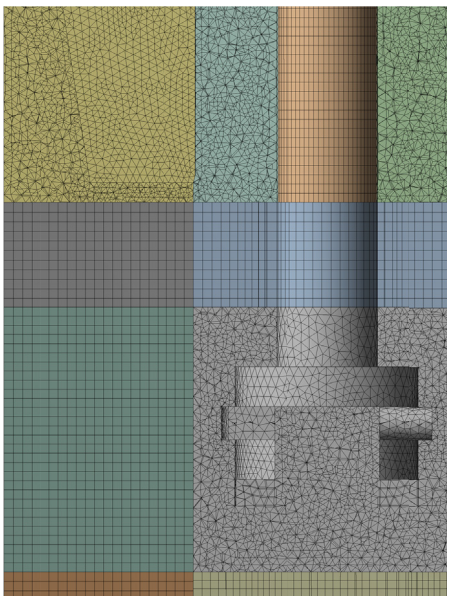

Fig. 2. Detail of computational mesh

2. Description of numerical model geometry and computational mesh

The object of CFD numerical modelling was a physical water model of a pilot ladle designated for refining of metals. The model for numerical modelling was constructed in the scale of 1: 1 to the physical model of refining ladle, as well as the rotor and breakwaters. The model geometry was formed according to the internal volume of the physical model of the reactor including fixation of positions of the rotor and breakwaters. The distance *h* of the lower edge of the rotor from the bottom of the reactor is an immersion of the rotor, which is variable depending on the modelled variants. The rotor diameter, adjusted for the needs of the pilot plant refining ladle, was 140 mm.

A combined computing mesh was created. The primary mesh tested for the given geometry consisted of nearly 2,500,000 computational elements. Initial simulations showed that this mesh was absolutely unacceptable since it was highly time-consuming. A non-stationary calculation of the simplest variant would take approximately four weeks when using normal computing capacity. It is also necessary to reflect the fact that the change in boundary conditions (bigger immersion, rising rpm) would result in an extension of the calculation time in the order of weeks. Therefore, the mesh consisting of the hexahedral and tetrahedral elements was used. The effort when preparing geometry for the mesh was to separate the areas of more complex shape (the area around the rotor and the breakwaters), for which an unstructured mesh consisting of tetrahedral elements was used. The remaining volumes with a simpler radial shape were filled with a structured mesh formed by hexahedral elements. The detail of computational mesh is shown in Fig. 2.

The distribution of geometry and use of a structured mesh has greatly reduced the number of elements of the computational mesh and improved its quality. The final size of the mesh reached 667,395 elements. Compared to the original mesh, it brought a significant reduction in the number of mesh elements; although this resulted in a slightly lower accuracy of the calculated results, however, due to the level of acceleration of the calculation and the size of the reactor, this inaccuracy was negligible and the mesh density allowed a sufficiently precise representation of the calculated shape of the surface, and the flow character in the reactor volume.

3. Modelling of turbulent and multiphase flowing

As it follows from the above objectives, numerical modelling of aluminium refining is a complex and complicated process. The solution involves the use of several models of different physical nature [13-15]. Numerical modelling of rotational degassing is based on the calculation of turbulent flow under simultaneously running rotation of the domain and the evolution of the gas, i.e. the interaction of the phase's melt. This program uses finite element method and finite volume method [15], and it contains models suitable for a numerical description of the investigated technology (see Table 1).

The turbulent flow was calculated as transient by a turbulent SST *k-ω* model using two equations. This model incorporates transport equations of turbulent quantities – turbulent kinetic energy *k* (2) and specific dissipation of turbulent kinetic energy *ω* (3) [16]. The turbulent model was complemented by a multiphase VOF model in an explicit formulation that was more suitable for unsteady flows.

$$\frac{\partial}{\partial t}(\rho k)+\frac{\partial}{\partial x_i}(\rho k u_i)=\frac{\partial}{\partial x_j}\left(\Gamma_k \frac{\partial k}{\partial x_j}\right)+G_k-Y_k+S_k \qquad (2)$$

$$\frac{\partial}{\partial t}(\rho \omega)+\frac{\partial}{\partial x_i}(\rho \omega u_i)=\frac{\partial}{\partial x_j}\left(\Gamma_\omega \frac{\partial \omega}{\partial x_j}\right)+G_\omega-Y_\omega+S_\omega \qquad (3)$$

where G_i represents the generation of k and ω, Γ_i is effective diffusivity of k and ω. Y_i is the dissipation of k and ω due to turbulence. S_i is user-defined source terms [16].

TABLE 1

Chosen model and their application

Model	File of application
Turbulent SST k-ω Model	Turbulent flow
Volume of Fluid Model	Multiphase flow (free surface)
Species Model	Diffusion of refining gas concentration (RTD Curves)
Discrete Phase Model	The size of bubble distribution in the melt

The aim of numerical modelling was to find the optimal method for computing and comparing the results of the measurement of the change in oxygen concentration (see ref. [12]) since in numerical modelling it is so far difficult to define the input volume concentration of oxygen in the model liquid. The intensity of the refining effect of inert gas blowing on oxygen removal under the simultaneous rotation of the domain was therefore primarily verified by monitoring the change in tracer concentration over time at the positions of the optical probes of the physical model and the rate of homogenisation of the liquid volume. The principle of calculating the change in concentration consisted of the definition of the passive scalar. The calculation was performed only in the liquid phase (water). For the calculation of the passive scalar, the Species Model was used, within the setting of which the following is defined: the tracer and the mixture, in which is propagate (water, oxygen). The steady flow field of the selected variant, calculated by the k-ω and the VOF model, was used again as the initial solution. The calculation included only the equation describing the propagation of the tracer (4) [16].

$$\frac{\partial}{\partial t}(\rho Y_i) + \nabla(\rho \vec{v} Y_i) = -\nabla \vec{J}_i + R_i + S_i \qquad (4)$$

where R_i is the net rate of production of species i and S_i is the rate of creation by addition from the dispersed phase plus any user-defined sources [16].

4. Initial and boundary conditions

To compare the results of physical and numerical modelling of refining technology, the properties of the aluminium melt were replaced by the physical properties of water. An overview of the chosen physical properties of the modelled media is given in Table 2.

TABLE 2

Physical properties

Medium	Density [kg×m^{-3}]	Dynamic viscosity [kg×m^{-1}×s^{-1}]
Air	1.225	1.7894×10^{-5}
Water	998	0.001003
Argon	1.6228	2.125×10^{-5}

5. Results and discussion

For verification of the functionality of the numerical model, four basic operational cases were defined, which were modelled also on a physical model (see ref. [12]). For these variants, two parameters were changed – the rotor rotational speed and rotor immersion. The setting of basic cases is shown in Table 3.

TABLE 3

Setting of model variants

Variant	Immersion of rotor, h, (mm)	Number of breakwaters, (-)	Rotational speed (rpm)
A10-35	100	2	350
A10-50	100	2	500
A15-35	150	2	350
A15-50	150	2	500

5.1. Velocity field and free surface

The velocity fields of the model variants are shown in Fig. 3, which compares the results of the velocity field of all variants. It can be seen that, at the same rotational speed and

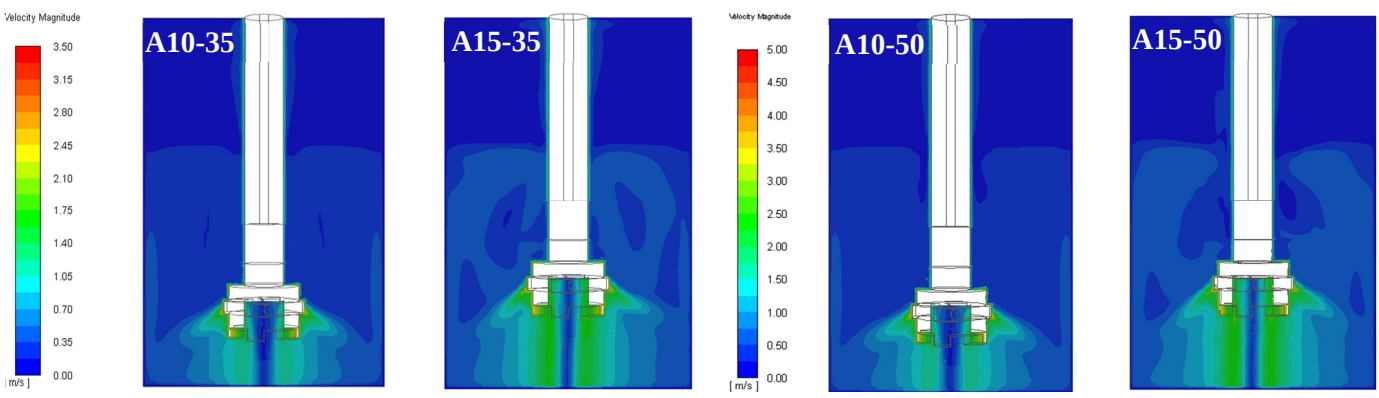

Fig. 3. Velocity field results of model variants

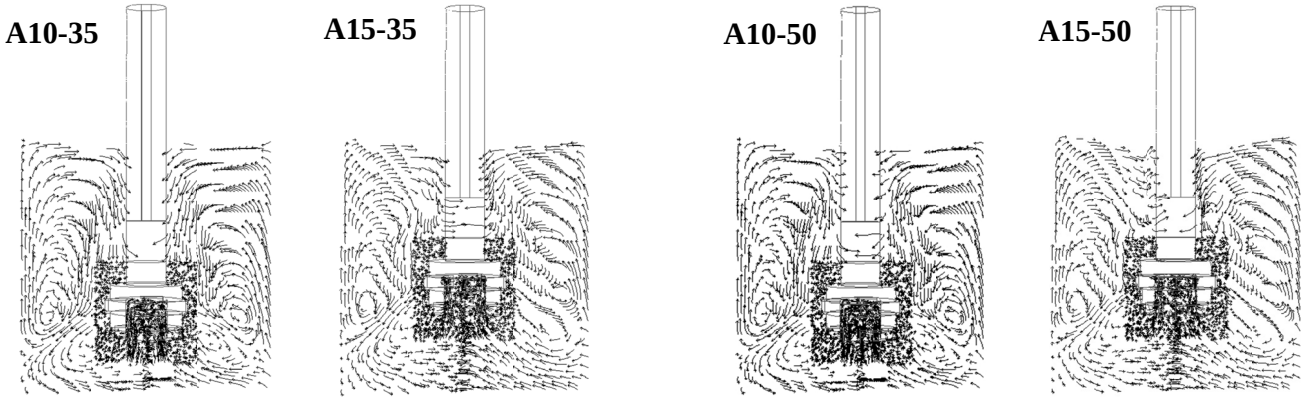

Fig. 4. Flow field results of model variants

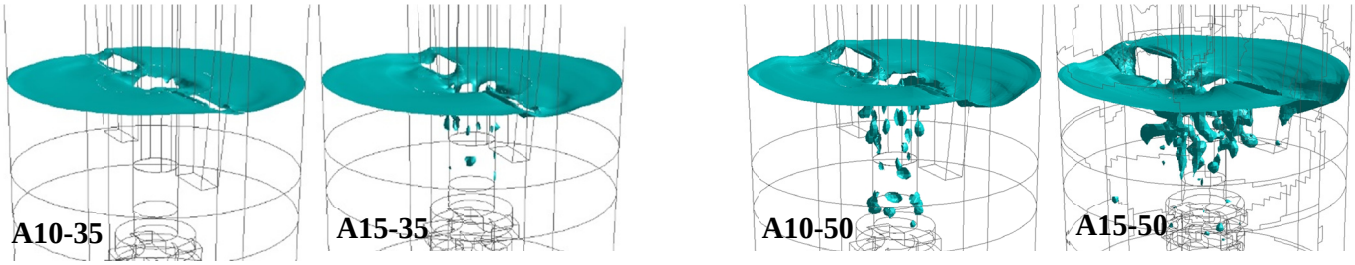

Fig. 5 Free surface results of model variant

different immersions, very similar velocity field in the reactor was achieved. Fig. 4 shows the pathlines and the phenomena of the water flow for the modelled variants. The comparison also shows a distinct visual consistency in the flow character that is noticeable in the region of the rotor that divides the rotating domains into the "lower" and "upper" circulating areas. Fig. 5 shows the shape of the free surface during the flow calculation of the four model cases. It is interesting that bubbles of the surrounding atmosphere retract into the melt due to rotor rotation, which intensifies with rising rotational speed and increasing rotor distance from the bottom (immersion *h*).

5.2. Modelling of hydrogen removal

The concentration curves of hydrogen removal (respectively oxygen removal) obtained by the numerical model is shown in Fig. 6. The diagrams monitoring the concentration change of the tracer in the ladle volume at two heights. The propagation of the concentration of the tracer was observed using monitors near the surface at the height of 0.425 m and at the bottom of the reactor at the height of 0.025 m, which corresponded to the positions of two optical probes on the physical model of the pilot plant. It can be seen that the lower monitors detect the dissolved substance earlier, which is related to the flow characteristic in the vicinity of the rotor. The top monitors detect the change in a concentration approximately 2 seconds later, while the volume fraction of the tracer reaches lower values. It is also apparent that with increasing rotor speed and distance from the bottom of the reactor (immersion *h*), the time of homogenisation of the reactor volume gets shorter. In the variant A10-35, the stabilisation was achieved after 17.5 seconds, whereas the variant A15-50 reached a homogeneous concentration already after 6 seconds.

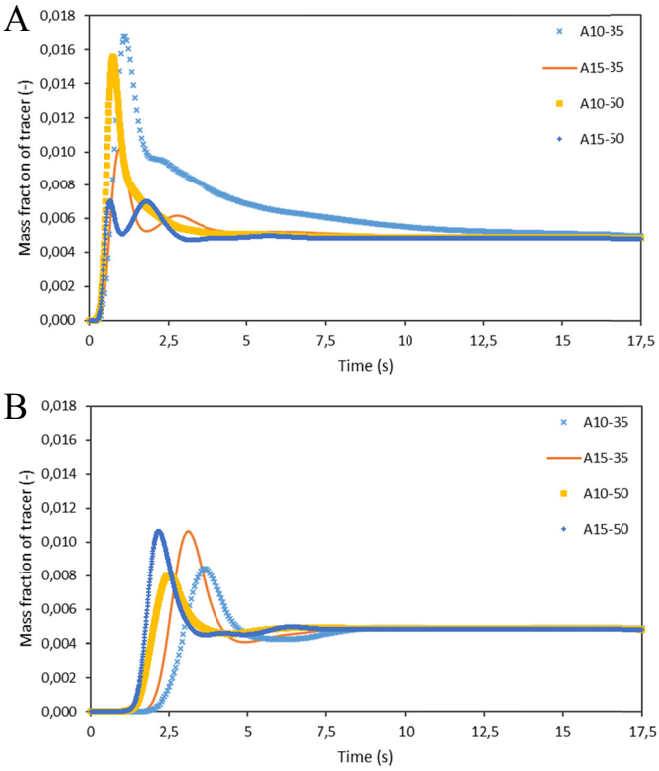

Fig. 6. Tracer mass fraction - RTD curve (A – lower monitor, B – top monitor)

5.3. Comparison of results from numerical and physical modelling

The RTD curves from numerical modelling correspond to the nature of the RTD (Residence Time Distribution) curves measured in the physical modelling of the melt refining within the frame of the research [17]. In this physical modelling, injection of NaCl was used for monitoring the change in concentration. At the same time, rotor rotations from 300 to 500 rpm were used, as well as argon flow rates of 15 l×min^{-1}. Although this modelling method does not define the actual time required to achieve the required minimum hydrogen content in the melt, it assumes that the fastest achieved and stabilised change in concentration represents the fastest homogenised melt volume in the ladle and determines the given variant as the most efficient also in industrial operating conditions during melt refining [17].

Consequently, the fastest and stabilised homogenisation times were monitored for the concentration curves from numerical modelling of versions presented in Table 3, and the correlation with the results of the physical model was studied (because the decrease in hydrogen content in aluminium melt during inert gas refining was simulated on the physical model by a decrease in the dissolved oxygen content in the model liquid (water), see ref. [12]). For primary numerically modelled versions, the results were consistent with the conclusions of the physical modelling on the model of the pilot plant for refining of the aluminium melt. Thus, with the increase of the rotational speed at a constant argon flow rate of 10 to 15 l×min^{-1}, the minimisation of the oxygen content, or homogenisation of the bath is achieved the most rapidly [12].

6. Conclusions

The paper presents the results of the numerical modelling of aluminium refining process using an inert gas. The conclusions stemming from the present research can be summarised in the following points:

- A pattern used for numerical simulation of this technology was the physical model of a pilot plant ladle for aluminium refining. This fact enables to confirm and to compare the results from physical and numerical modelling.
- The calculation time of CFD analysis for the given technology is strongly dependent on the size of the computing mesh. Reduction of cells of the computing mesh can shorten the calculation time even to the order of weeks.
- The two-equational SST k-ω model was selected for calculation of the flow. The behaviour of the free surface was described using a multiphase VOF model. Calculation of RTD curves was performed using the Species Model.
- The reactor velocity field is dependable on rotation speed. No significant change in flow velocity in the reactor was observed when increasing immersion of the rotor.
- The character of the flow in the reactor shows similar behaviour in all modelled variants regardless of the rotor rotational speed and its immersion. In all variants, the character of the flow divided the volume of water in the ladle into the upper and lower circulating areas. This phenomenon was follow also during the physical modelling of the process.
- The results of the VOF model showed that the bubbles from the surrounding atmosphere were retracted into the water volume in the reactor. The intensity of retracting the ambient atmosphere is intensified with the increasing rotational speed of rotor and its immersion. This phenomenon should be further studied, and should be verified during the physical modelling of the given process.
- Physical and numerical modelling of the concentration curves of the tracer was performed. Concentration curves calculated by the numerical model approximated the curves measured during physical modelling when the conductivity probes were used to monitor the concentration. This method does not accurately define the actual time necessary for reaching the minimum hydrogen content in the melt, but it is possible to define the degassing efficiency under the given boundary conditions. Moreover, the results obtained were consistent with the measurement of the oxygen concentration on the physical model with the use of optical probes, which corresponded to the H concentration in the aluminium melt in industrial operating conditions.
- From the results of the physical and numerical modelling of the defined variants, it can be assumed that with the increasing rotational speed and increasing distance of the rotor from the bottom, the refining intensity is increasing.

Determination of the intensity of degassing will be given additional attention in numerical simulations. For example, it is worth considering to define the initial oxygen content in points in the volume of water.

Acknowledgements

The work was created under the support of the Czech Ministry of Industry and Trade within the frame of the programme TRIO in the solution of the projects reg. No. FV10080 "Research and Development of Advanced Refining Technologies of Aluminium Melts for Increase in Product Quality". This paper was created with the financial support from the Moravian-Silesian Region budget under the program "Support for Science and Research in the Moravian-Silesian Region" (RRC/10/2017), Student Grant Competition No. SP2019/148 and SP2019/43. This work was supported by The Ministry of Education, Youth and Sports from the Large Infrastructures for Research, Experimental Development and Innovations project „IT4Innovations National Supercomputing Center – LM2015070".

This paper was partially created with the financial support of Polish Ministry for Science and Higher Education under internal grant BK221/RM0/2018 for Faculty of Materials Engineering and Metallurgy, Silesian University of Technology, Poland.

REFERENCES

[1] D. Vojtěch, Kovové materiály. VŠCHT. Praha (2006).

[2] J. Roučka, Metalurgie neželezných slitin. CERM, Brno (2004).

[3] T. Merder, M. Saternus, P. Warzecha, Arch. Metall. Mater. **59** (2), 789-794 (2014). DOI: 10.2478/amm-2014-0134.

[4] O. Migraux, D. Ablitzer, E. Waz, J. P. Bellot, Metall. Mater. Trans. B. **40B**, 363-375 (2009). DOI: 10.1007/s11663-009-9233-3.

[5] Y. Liu, T. Zhang, M. Sano, Q. Wang, X. Ren, J. He, Trans. Of Nonferrous Metals Society of China **21**, 1896-1904, (2011). DOI: 10.1016/S1003-6326(11)60947-3.

[6] L. Zhang, X. Lv, A. Tryg Torgerson, M. Long, Mineral processing & Extractive Metall. Rev. **32**, 150-228 (2011). DOI: 10.1080/08827508.2010.483396.

[7] E.R. Goméz, R. Zenit, C.G. Rivera, G. Trápaga, M.A. Ramírez-Argáez, Metall. Mater. Trans. B, **44B**, 423-435 (2013). DOI: 10.1007/s11663-012-9774-8.

[8] M. Hernández-Hernándes, J.L. Camacho-Martínez, C. Gonzáles-Rivera, M.A. Ramírez-Argáes, J. Mater. Process. Tech. **236**, 1-8 (2016). DOI: 10.1016/j.jmatprotec.2016.04.031.

[9] V. S. Warke, s. Shankar, M.M. Makhlouf, J. Mater. Process. Tech. **168**, 119-126 (2005). DOI: 10.1016/j.jmatprotec.2004.10.016.

[10] A. Ghosh, Secondary Steelmaking: Principles and Applications. CRC Press, Boca Raton (2001).

[11] T. Myslivec, Fyzikálně chemické základy ocelářství. SNTL, Praha (1971).

[12] J. Čarvaš, MSc thesis, Physical Modelling of Melt Degassing in the Rafination Ladle, VŠB-TU Ostrava, Ostrava, Czech Republic (2018).

[13] J.N. Reddy, D.K. Gartling. The finite element method in heat transfer and fluid dynamics. CRC Press, Boca Raton (2010).

[14] J.H. Spurk, N. Aksel, Fluid Mechanics, Springer, Berlin (2008).

[15] ANSYS FLUENT 19.2 User´s Guide. (2018), ANSYS, Inc.

[16] ANSYS FLUENT 19.2 Theory Guide. (2018), ANSYS, Inc.

[17] M. Saternus, T. Merder, Metals **8** (9), (2018). doi:10.3390/met 8090726.